*Midlands State University Journal of Science, Agriculture and Technology Volume 4(1), 2013*

# Above-ground woody biomass estimation in a communal African savanna woodland using microwave remote sensing based approach

***[1] C. Paradzayi, [2]H. J. Annegarn and [3]C. Schmullius***

*[1] Department of Surveying and Geomatics, Midlands State University, Gweru, Zimbabwe*
*[2] Department Geography, Environmental Management and Energy Studies, University of Johannesburg, Johannesburg, South Africa*
*[2] Department of Earth Sciences, Friedrich Schiller University, Jena, Germany*
[2] ***Corresponding author:*** *Email: cparadzayi@gmail.com, Mobile: +263 774 003 137*

## Abstract

*Estimations of available fuelwood resources in communal savanna woodlands are widely based on conventional terrestrial and optical remote sensing approaches, which are constrained by limited geographic footprints and the use of leaf area indices and normalised difference vegetation indices, as surrogates for above ground biomass. As a result, reliable information about the location and estimated quantities of available woody biomass is scarce at local, national and global scales. Recent developments have shown that classification of backscatter information contained in full polarimetric radar retrievals from satellite borne sensors can discriminate between woody and non-woody vegetation. The intensity of the backscattered signal has been shown to be sensitive to above ground biomass density. However, no such studies have been reported across African savanna woodlands. This paper presents a study which used full polarimetric ALOS PALSAR retrievals to map and quantify fuelwood resources in communal savanna woodland in Welverdiend village, South Africa. Unsupervised entropy/alpha angle Wishart classification and maximum likelihood classification procedures are used to characterise the scattering classes from the ALOS PALSAR retrievals into eight major terrain scattering mechanisms. Five vegetation classes (random anisotropic, forest double bounce, vegetation, dihedral and dipole) are identified that are closely related to backscattering from woody vegetation components. Correlations between backscatter intensities acquired under dry and wet conditions with above-ground biomass densities estimated from field surveys are investigated to derive equations for predicting biomass densities. The regression analysis supports findings of similar studies where the HV backscatter intensity showed moderately strong relationship (R2>0.6) with above ground biomass densities. The inverted regression equations were used to estimate the biomass densities for areas covered with woody vegetation. Knowledge about the location and distribution of woody biomass has significant implications for fuelwood management and carbon sequestration initiatives. A combination of woodland management interventions, coupled with the transition to modern energy sources, has the potential of turning communal woodlands into carbon sinks.*

**Keywords:** full polarimetric, synthetic aperture radar, above-ground woody biomass, fuelwood, ALOS PALSAR, savanna woodlands

## Introduction

Communal woodlands provide the bulk of woody biomass used for domestic cooking and heating energy in most rural and low-income urban communities in sub-Saharan Africa. The scarcity of contemporary information on above ground woody biomass stock in communal African savanna woodlands and on rates of production and regeneration is posing a major challenge in modelling domestic energy demand and supply at local levels (Banks et al, 1996; Von Maltitz & Scholes, 1995). At the same time, the exploitation of traditional biomass resources, for cash and mercantile purposes, is leading to accelerated losses of carbon sinks, natural forests and biodiversity, as well as creating local scarcity of fuelwood. Carbon stocks in communal woodlands are becoming crucial input for the reporting requirements of international conventions such as Reducing Emissions from Degradation and forest Deforestation (REDD) (Mitchard et al., 2009; Ryan et al., 2011; Woodhouse et al., 2009).

Ground surveys and optical remote sensing approaches for mapping and estimating biomass are well documented. Ground based techniques are tedious, time-consuming and have limited geographic coverage (Bombelli et al., 2009; Das & Ravindaranth, 2007; Lu, 2006). Optical remote sensing approaches are affected by cloud cover and rely on proxies to estimate biomass. On the other hand, synthetic aperture radar remote sensing techniques have been used successfully to estimate above-ground biomass in several studies of boreal and temperate forests (Rauste, 2005; Santoro et al., 2009). However, there is no widespread application of full polarimetric synthetic aperture remote sensing approaches to estimate woody biomass as indicated by the scarceness of relevant literature, especially over the African continent. The few available studies have used fine beam dual polarisation retrievals (Ryan et al., 2011; Mitchard et al., 2009; Woodhouse et al., 2009) as opposed to full polarimetric retrievals.

Optical remote sensing approaches use leaf area indices and normalised difference vegetation indices as surrogates for woody biomass that are affected by seasonality and plant senescence. These indices are not directly related to the interactions of the optical signals with tree trunks or branches that constitute the bulk of above ground woody biomass. On the other hand, microwave retrievals are insensitive to weather conditions and the microwave signal interacts directly with tree trunks and branches. There has been a rapid evolution of techniques which can decompose the signals arising from interactions of microwave signals with vegetated terrain surfaces, derived from synthetic aperture radar (SAR) retrievals (Cloude & Pottier, 1997; Freeman & Durden, 1998; van Zyl, 1989; Yamaguchi et al., 2005). In particular, the decomposition technique developed by Cloude and Pottier can extract entropy, alpha angle and anisotropy parameters from full polarimetric retrievals (Cloude & Pottier, 1997). These parameters have been used with the unsupervised classifier to identify terrain scattering mechanisms. It has been shown that woody vegetation is associated with anisotropic scattering, forest double bounce, random anisotropic scattering, dihedral and dipole scattering classes (Lee & Pottier, 2009; Touzi et al., 2004).

The intensity of the backscattered signal from synthetic aperture radar remote sensing retrievals has been correlated with above-ground biomass in studies of boreal and temperate biomes. Several studies have established the relationship between above-ground biomass density and backscatter intensity for savanna woodlands in Australia (Collins et al., 2009; Liang et al., 2005; Lucas et al., 2006; Lucas et al., 2004; Lucas et al., 2002), Brazil (Narvaes et al., 2007; Santos et al., 2002), Belize (Viergever, 2008) and Africa (Ryan et al., 2011; Mitchard et al., 2009; Woodhouse et al., 2009). Results from these studies have shown relatively strong correlation between above-ground biomass density and backscatter intensities from L-band HH and HV polarised retrievals. Saturation levels of the backscatter intensity to biomass for L band retrievals ranges between 60 t ha-1 and 150 t ha-1 (Mitchard et al., 2009; Santoro et al., 2006; Santos et al., 2002; Viergever et al., 2007). The HV backscatter retrievals are least affected by forest type, and are not sensitive to ground moisture, slope and roughness variations (Leckie, 1998).

This paper presents the application of full polarimetric ALOS PALSAR retrievals in mapping and estimating above ground woody biomass resources in semi-open African savanna, demonstrated on a case study for Welverdiend village in the Mpumalanga Province of South Africa. The approach combines classification procedures to extract terrain features, based on their polarimetric scattering mechanisms, and regression analysis to produce woody biomass distribution maps and related biomass estimates.

**Description of case study area**

In 2006, the VW Foundation funded the BioModels project, a multi-institutional and interdisciplinary bioenergy modelling project that sought to provide stakeholders with quantitative information on available woody biomass resources and their utilisation in selected rural communities in South Africa, Mozambique and Zambia3. In South Africa, Welverdiend village, in the Mpumalanga province was chosen as an existing research site with extensive local data on utilisation of heavily depleted woodland resources. The selection of Welverdiend village was also influenced by the availability of digital spatial datasets, aerial photographs, high resolution digital elevation models and meteorological information.

The savanna woodlands in the case study site are spatially heterogeneous, with varying vertical and crown structures (Campbell et al., 1996). The savanna woodlands are characterised by discontinuous woody crown cover taller than 2 m, with herbaceous cover dominated by varying grass densities (Nangendo, 2005; Rutherford et al., 2006; Scholes & Archer, 1997; White, 1983). Savanna woodlands have an assortment of deciduous fine leafed and broad-leafed trees, interspersed with seasonally wet grassy depressions (Campbell et al., 1996). The Mimosaceae family dominates fine-leafed savannas, found in low-lying arid areas with well-drained and nutrient rich soils. Broad-leafed savannas are dominated by trees from the Combretaceae and Cesalpinoideae families, with dominant Brachystegia, Julbernardia and Isoberlinia species occurring mostly in high rainfall areas with well-drained, nutrient-poor soils (Rutherford et al., 2006; Scholes, 1997).

## Methods

An integrated approach was adopted that includes field assessment surveys of woody biomass in test plots, extraction of normalised backscatter intensities from POLSAR retrievals and predictive analysis (Figure 1).

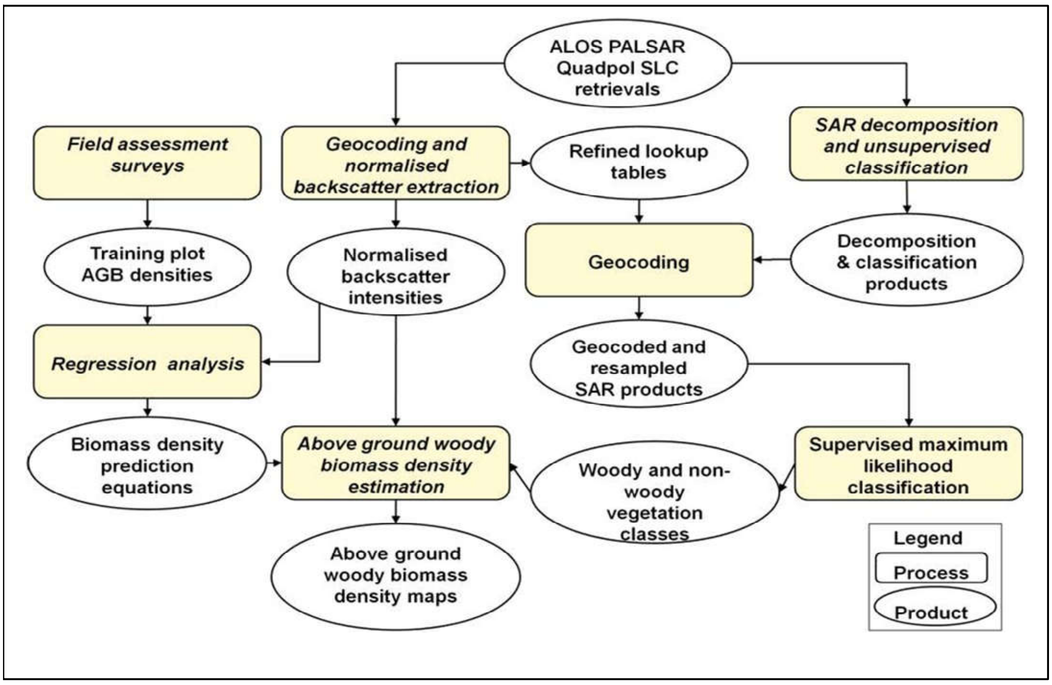


***Figure 1:** Overall above-ground woody biomass estimation procedure*

### 1.1 SAR retrievals

The study was carried out using full polarimetric ALOS PALSAR level 1.1 retrievals acquired in 3 November 2008 (PSR_MMC_TP_0003140001) and 6 May 2009 (PSRMMC_TP_0004483001) over Welverdiend village (24°30′ S, 31°16′ E). The images were acquired courtesy of the European Space Agency (ESA) under the Principal Investigator Project (CIP.6143) on "Quantifying above ground woody biomass in communal African savanna woodlands using fully polarimetric L-band data". Analysis of the meteorological information indicate wet conditions for retrievals acquired in November 2008 and dry conditions for the May 2009 acquisitions. An average of 12mm of rainfall was recorded prior to the November acquisition while no rain was recorded ten days before the May acquisition.

### 1.2 Field assessment surveys

Comprehensive field assessment surveys were undertaken to measure biomass quantities in selected sampling plots to provide training data for estimating above-ground woody biomass from remote sensing approaches. The surveys included training plot selection, tree parameter measurement and above-ground biomass estimation at plot level. The locations of training plots were dictated by the broader needs of the VW Foundation Biomodelling project and were confined to areas where villagers collect fuelwood resources. Training plots are strategically located along linear transects, radiating from the centre of Welverdiend village, to capture changes in vegetation with the increased walking distances from the village. Training plots are located at the near, mid and far range from the centre to span a range of biomass densities, from lowest to highest. Plots in the near range were located at a minimum distance of 350 m from any households or agricultural fields. Twenty four training plots were identified from visual interpretation of available optical satellite imagery, aerial photographs and information about the village boundaries, households and agricultural fields.

Topographic mapping and baseline sampling approaches were used to sample trees in training plots. The topographic mapping approach uses reference points that were established using an OmniSTAR$^{\grave{O}}$ real time differential Global Positioning System (GPS) system. Surveying instruments (Total Station) were used to take distance and direction measurements from the reference points to trees marking the extent of training plots which are used to compute bounding coordinates. The centre points of the baseline sampling approach were located using a hand held GPS receiver. The topographic mapping approach employed a radiation method to establish the geographic position and height of every sampled tree by observing the zenith angle, slope distance and direction from a Total Station instrument set up over a reference point (Ghilani & Wolf, 2008; Uren & Price, 2010). In the baseline sampling approach, a 50 m baseline was used with 5 m wide transects taken at 5 m intervals perpendicular to the baseline. For each sampled tree, diameter at ankle[1] height was recorded. The biomass for each sampled tree is computed from the diameter at ankle height measurements and allometric equations for savanna woodlands.

[1] *The growth habit of many savanna species is multi-stemmed from ground level, so the conventional approach of measuring stem diameter at chest height is not appropriate in these woodlands.*

$$\text{Biomass} = 0.035 * D^{2.5}$$

**Equation 1**

where D is the diameter at ankle height (Netshiluvhi & Scholes, 2001).

## 1.1 Regression analysis

ALOS PALSAR retrievals were processed to extract normalised backscatter intensities after accounting for topographic distortions (such as layover, foreshortening and shadow effects) (Lauknes & Malnes, 2004). The processing chain used a suite of GammaÒ and PolsarproÔ remote sensing software packages. The processing chain to extract normalised backscatter intensities from ALOS PALSAR retrievals included: calibration and multi-looking; resampling of the digital elevation model; simulation of SAR image (by taking into account the topography of the area under investigation); creation of a *lookup table* for geocoding the SAR retrievals to map projection (cartographic) systems; and topographic normalisation (Knuth, 2008). The normalised backscatter intensity is converted to backscatter coefficient (sigma nought) using Equation 2.

$$\text{Sigma nought } (\sigma°) = 10 \text{ x } \log_{10} (\sigma)$$

**Equation 2**

where ó is the normalised backscatter intensity.

The logarithmic relationship between backscatter intensity and above ground biomass density was determined from the regression analysis of the correlation between the ground inventory biomass measurements and sigma nought (ó°) of HH, HV and VV retrievals. The twenty four training plots provided limited training dataset, hence, a bootstrapping approach was introduced to generate a large sample using the technique of sampling with replacement (Moore *et al*., 2009; Mutanga *et al*., 2005; Saatchi *et al*., 2007a). The resampled datasets were regressed against the training plot biomass estimates to determine the resampled dataset with the highest coefficient of determination. The regression equations are inverted to predict the above-ground biomass density for given backscatter intensity from each particular polarisation channel. In general, the predicted above-ground biomass density is calculated from the Equation 3:

$$AGB_{\rho} = e^{\left(\sigma^{o} + \sigma_{c}^{o}\right)/K}$$

**Equation 3**

where $AGB_{ñ}$ is the required above-ground biomass density, σ° is the mean sigma nought value for SAR pixels, $\sigma_c^0$ is a constant associated with the sigma nought from a specific polarisation channel, and *K* is the slope of the logarithm regression for the above-ground biomass density for the respective acquisition channel. The biomass prediction equations were used with the training plot AGB densities to determine their associated root mean square errors.

### 1.2Polarimetric decomposition and classification

Algorithms developed by (Cloude & Pottier, 1997) and (Freeman & Durden, 1998) are used to decompose the full polarimetric ALOS PALSAR retrievals and to identify terrain scattering mechanisms using a combination of unsupervised classification and the Maximum Likelihood Classification procedures. The Cloude-Pottier decomposition retrieves entropy, alpha angle and anisotropy elements and classifies from full polarimetric radar retrievals into physical scattering mechanisms by segmenting the H/a plane (Cloude & Pottier, 1997). The entropy/alpha segmentation plane is used to identify eight scattering classes using the unsupervised Wishart classification procedure. The Freeman decomposition algorithm extracts double, volume and surface scattering which are used to generate RGB composites over ALOS PALSAR scenes (Freeman & Durden, 1998; Zhang *et al.*, 2008). The RGB composites represent double bounce, volume and surface scattering mechanisms as red, green and blue, respectively. Regions with woody vegetation appear in shades of green on the composite image.

The supervised maximum likelihood classification procedure uses samples of terrain scattering features from unsupervised Wishart classification procedure as training classes to extract refined classes from the RGB composite of the Freeman decomposition elements. The training datasets are subjected to the Jeffries-Matusita separability test (Richards & Jia, 2006; Riedel *et al.*, 2008) before running the maximum likelihood classification procedure.

### 1.3 Woody biomass density estimation

Above-ground woody density is estimated from normalised backscatter intensity retrievals and biomass density prediction equations. The woody vegetation map generated from the supervised maximum likelihood classification procedure is used to mask areas of interest on the raster image of derived biomass densities. The resulting densities are classified into classes with 20 t $ha^{-1}$ increments. A similar classification approach was adopted by (Saatchi *et al.*, 2007b). The mean values of the biomass density classes are used to compute the available above-ground biomass resources.

## 2 Results

### *2.1 Training plot biomass densities*

Individual tree biomass was estimated by applying allometric equations to tree diameters measured at ankle height. The plot biomass density was then calculated from the sum of the sampled tree biomass divided by the areal extent of each training plot. The biomass densities obtained from the field assessment survey (Welverdiend village) are shown in Table 1.

**Table 1:** Above-ground biomass densities from field assessment surveys (Welverdiend village)

| Training plot | AGB density (t ha$^{-1}$) | | Training plot | AGB density (t ha$^{-1}$) |
|---|---|---|---|---|
| N1 | 1.7 | | SE2 | 2.8 |
| N2 | 1.5 | | SE3 | 7.0 |
| N3 | 0.8 | | W1 | 24.9 |
| NE1 | 5.5 | | W2 | 5.8 |
| NE2 | 4.1 | | W3 | 14.5 |
| NE3 | 0.7 | | W4 | 7.6 |
| NW1 | 6.0 | | W5 | 80.4 |
| NW2 | 3.9 | | North 2* | 0.8 |
| S1 | 1.5 | | North 3* | 2.8 |
| S2 | 45.3 | | West 6* | 9.9 |
| S3 | 4.7 | | North 1* | 1.8 |
| SE1 | 11.1 | | WLFC* | 17.0 |

** Training plots sampled using topographic mapping. Baseline sampling was used for the other training plots*

The range of biomass densities was consistent with reported densities for savanna woodlands (Bombelli *et al.*, 2009; Chidumayo *et al.*, 2002). The case study area is characterised by relatively short trees with an average height of 3 m. The bulk of sampled plots have relatively low biomass levels due to extensive exploitation of woody biomass resources surrounding Welverdiend village. As a result, the regeneration of trees is constrained and they do not have an opportunity to grow to larger size. In general, the remaining taller trees are fruit bearing trees protected by custom; these fruiting trees are not used for fuelwood purposes.

### 1.1 Backscatter intensity and above-ground biomass relationship

Normalised backscatter intensities for the training plots were extracted from ALOS PALSAR retrievals after geocoding and correcting for topographic effects. The normalised backscatter intensities were converted to their sigma nought values (Table 2) and regressed against the biomass density estimates from the field assessment surveys.

**Table 2** Mean sigma nought values for training plots around Welverdiend village

| Training plot | AGB (t ha$^{-1}$) | Sigma nought (dB) | | | | | |
|---|---|---|---|---|---|---|---|
| | | 3 November 2008 | | | 6 May 2009 | | |
| | | HH | HV | VV | HH | HV | VV |
| N1 | 1.7 | -9.5 | -15.9 | -10.9 | -12.3 | -18.7 | -13.7 |
| N2 | 1.5 | -11.2 | -18.4 | -12.4 | -12.7 | -18.7 | -14.4 |
| N3 | 0.8 | -9.4 | -20.1 | -12.0 | -14.8 | -20.7 | -15.2 |
| NE1 | 5.5 | -12.7 | -21.5 | -12.2 | -17.3 | -23.2 | -17.9 |
| NE2 | 4.1 | -11.6 | -21.5 | -11.2 | -16.1 | -24.2 | -16.3 |
| NE3 | 0.7 | -10.5 | -20.2 | -9.8 | -16.4 | -21.2 | -15.7 |
| NW1 | 6.0 | -6.2 | -14.9 | -11.0 | -11.5 | -17.6 | -12.4 |
| NW2 | 3.9 | -8.9 | -19.5 | -10.5 | -13.7 | -19.6 | -12.5 |
| S1 | 1.5 | -9.3 | -18.9 | -12.4 | -13.2 | -20.5 | -15.0 |
| S2 | 45.3 | -8.6 | -17.9 | -10.9 | -11.6 | -18.4 | -13.1 |
| S3 | 4.7 | -9.0 | -17.5 | -10.0 | -11.3 | -17.4 | -12.4 |
| SE1 | 11.1 | -9.5 | -15.5 | -10.0 | -11.4 | -17.1 | -13.7 |
| SE2 | 2.8 | -8.6 | -17.6 | -11.0 | -12.3 | -19.4 | -12.6 |
| SE3 | 7.0 | -9.1 | -18.3 | -9.2 | -13.0 | -18.3 | -13.6 |
| W1 | 24.9 | -6.1 | -14.7 | -9.2 | -11.9 | -18.6 | -11.8 |
| W2 | 5.8 | -7.0 | -16.3 | -9.7 | -12.5 | -18.6 | -13.1 |
| W3 | 14.5 | -8.6 | -17.0 | -11.7 | -13.3 | -17.9 | -13.0 |
| W4 | 7.6 | -8.3 | -15.8 | -10.0 | -12.0 | -18.6 | -13.4 |
| W5 | 80.4 | -7.6 | -14.4 | -9.4 | -12.0 | -18.9 | -13.5 |
| North 2 | 0.8 | -9.9 | -18.2 | -11.7 | -13.0 | -19.0 | -15.0 |
| North 3 | 2.8 | -8.5 | -20.0 | -11.7 | -14.5 | -21.0 | -14.8 |
| WLFC | 17.0 | -7.6 | -17.8 | -10.3 | -12.8 | -20.6 | -14.6 |
| West 6 | 9.9 | -7.0 | -14.1 | -9.4 | -11.4 | -16.3 | -12.8 |
| North 1 | 1.8 | -10.3 | -15.5 | -10.9 | -12.7 | -19.7 | -14.4 |

Results from the November 2008 HH, HV and VV polarisation retrievals yielded relatively moderate correlation coefficients of 0.51, 0.48 and 0.50 (corresponding $R^2$ values of 0.26, 0.23 and 0.24) respectively. The correlation coefficients for the May 2009 HH, HV and VV polarisations retrievals were 0.44, 0.32 and 0.43, respectively (with corresponding $R^2$ values of 0.19, 0.10 and 0.18). The results seem to indicate that there is moderate correlation between backscatter intensity and above ground biomass density for this region. The moderate correlations may be due to the limited number of training plots that did not represent the full biomass density spectrum, coupled with PALSAR image georeferencing errors due to the small size of the sampled training plots.

The training dataset above was subjected to bootstrapping and resampled datasets with the highest coefficient of determination for each polarisation channel were identified. The results of the regression analysis between the bootstrapped results and sigma nought values are shown in Figure 2.

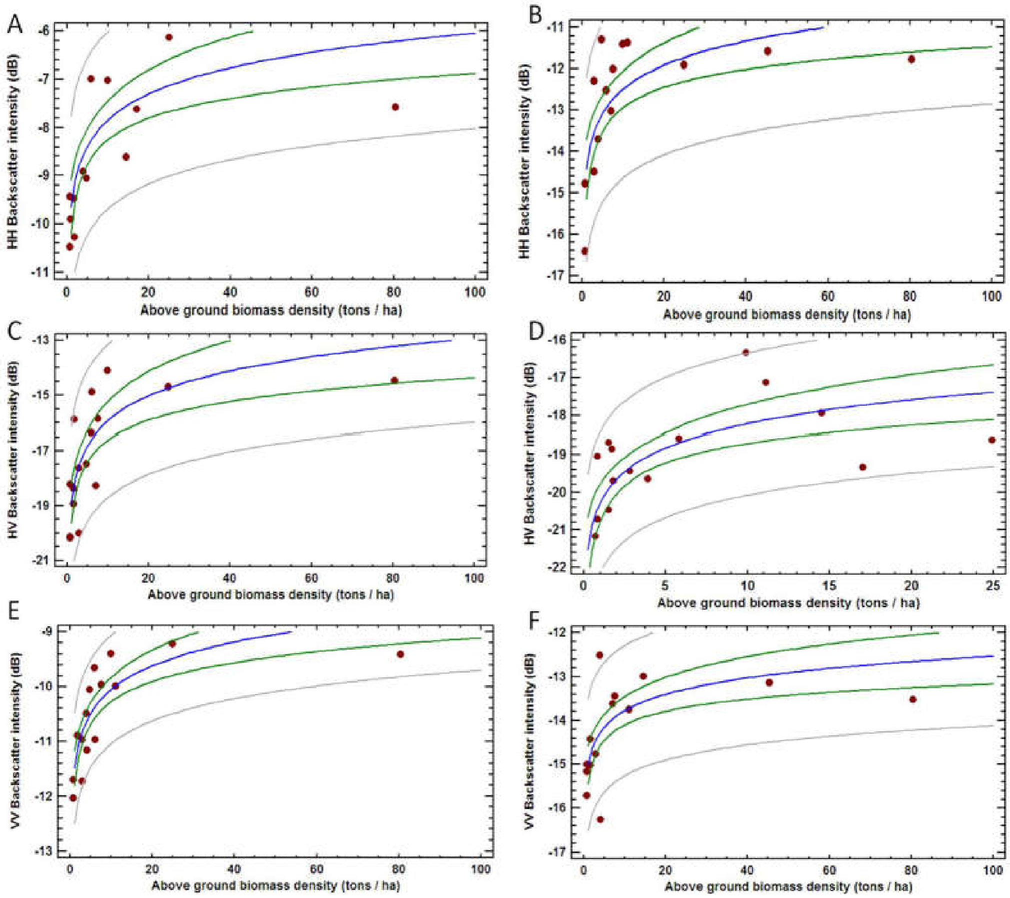


***Figure 2 Backscatter intensity and above-ground biomass density correlation diagrams for wet and dry condition acquisitions***

*The central line shows regression equation or line of best fit, which was used to predict the backscatter intensity (dependent) values given the above-ground biomass density (independent variable). The inner and outer bounds indicate one and two standard deviation limits (66% and 95% confidence intervals, respectively).*

The training dataset had few plots in the medium to high end of the biomass density spectrum. As a result, the relationships are characterised by cluster of points on the lower end of the biomass density spectrum. The HH and HV retrievals acquired under dry conditions (May 2009) show relatively poor correlations with above-ground biomass densities. The regression equations were inverted to derive biomass density prediction equations according to Equation 3. A summary of the fitted parameters to biomass density prediction equation are shown in Table 3.

Table 3 Summary of the results of regression analysis for Welverdiend training dataset

| Acquisition | Polarisation | $\sigma_c^0$ (dB) | K | R | R2 | SE (dB) |
|---|---|---|---|---|---|---|
| | HH | -9.7 | 0.8 | 0.80 | 0.65 | 0.9 |
| Nov 2008 | HV | -18.9 | 1.3 | 0.82 | 0.68 | 1.3 |
| | VV | -11.5 | 0.6 | 0.87 | 0.76 | 0.5 |
| | HH | -14.4 | 0.8 | 0.78 | 0.60 | 1.0 |
| May 2009 | HV | -20.3 | 0.9 | 0.80 | 0.63 | 0.9 |
| | VV | -15.0 | 0.5 | 0.78 | 0.61 | 0.7 |

November 2008 – summer, May 2009 – winter

The results show the general trend expected of the relationship between backscatter intensity and biomass density. The relationship between HV retrievals and biomass densities appeared relatively strong for both wet and dry condition acquisitions, with R2 values of 0.68 and 0.63 respectively. The result was consistent with previous studies that had found significant correlation between L-band HV backscatter and above-ground biomass density (Milne et al., 1999; Mitchard et al., 2009; Rauste, 2005; Watanabe et al., 2006). Mitchard et al. (2009) used ALOS PALSAR retrievals acquired using the fine beam dual (FBD) polarisation mode. The HV signal interacts with leaves, small branches and tree stems, but is least affected by forest type, topography and ground surface conditions such as local slopes, roughness and soil moisture (Prakoso, 2006). It has been observed that L-band HV retrievals have greater dynamic range; hence, greater sensitivity to differing ranges of biomass than HH or VV retrievals (Le Toan et al., 2004; Lucas et al., 2006).

HH, HV and VV retrievals observed under wet conditions showed relatively high correlation with biomass (R2 values greater than 0.65), possibly because of the moisture content in both soil and vegetation that resulted in strong backscatter returns for all channels. However, the backscatter intensities acquired using the HH and VV channels during the dry condition showed moderate correlation between observed biomass densities. The moderate correlation coefficient for the HH polarisation was possibly because of the absence of soil moisture to enable double bounce backscattering of HH signals from trunk and ground interaction. Biomass prediction equations for HV polarisation retrievals were adopted for the estimation of woody biomass resources in the case study villages.

***Terrain feature classification***

The ALOS PALSAR retrievals have of 9.37 m pixel spacing in slant direction and an incidence angle of 23.1°, resulting in a ground range resolution of 23.9 m. The pixel spacing in the azimuth direction is 3.52 m. A multi-look ratio of 1:7 (one ground range pixel to seven azimuth direction pixels) was used to resample the ALOS PALSAR retrievals to 25 m pixels. The ALOS PALSAR data products were resampled using the nearest neighbour algorithm to preserve the original data values as much as possible (Knuth, 2008; Werner et al., 2002).

The characterisation of the entropy/alpha segmentation plane resulted in eight scattering classes by discriminating scattering from surface, volume and double bounce mechanisms along the alpha and entropy axes (Cloude & Pottier, 1997; Touzi et al., 2004). The scattering from natural vegetation and some built up areas is associated with volume and multiple scattering corresponding to dense, mixed and sparse woody vegetation classes (multiple and volume scattering components). Scattering over forested areas is dominated by volume diffusion while urban areas are mainly characterized by double bounce scattering.

The training classes from the unsupervised classification were used as training dataset for the supervised maximum likelihood classification procedure (Figure 3). An overall classification accuracy of 87% and a kappa coefficient of 0.77 were obtained for the classified image (using scene acquired in November 2008 over Welverdiend Village).

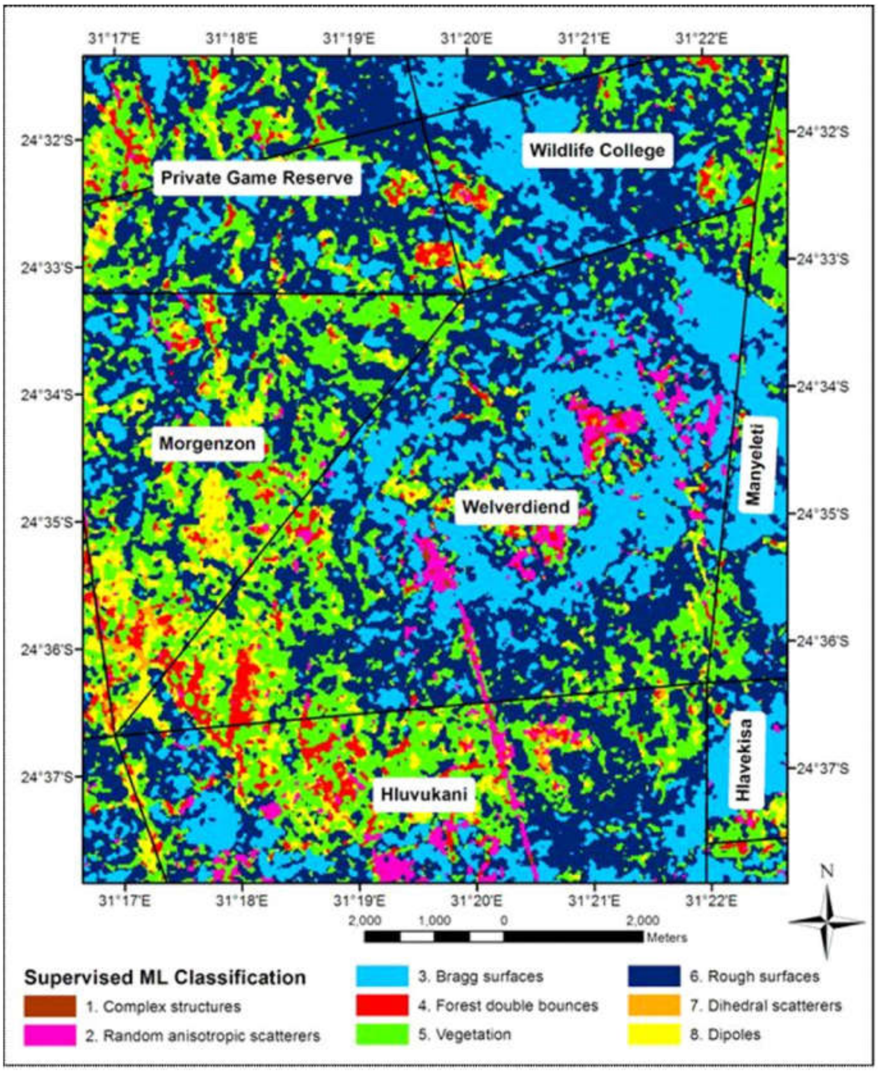


***Figure 3*** Supervised maximum likelihood classification results of ALOS PALSAR PSR_MMC_TP__0003140001 scene acquired in November 2008

The classification results show that built up areas are characterised by complex scattering elements. Bare areas (including open grasslands) and agricultural fields are dominated by rough and Bragg surfaces. This is evidenced on the eastern side of Welverdiend village, which is dominated by basalt and gabbro derived soils. Basalts are open grasslands characterised by heavy clayey soils (Mutanga et al., 2004). Gabbro derived soils support open savanna vegetation characterised by dense grass cover with scattered trees and shrubs[2]. This area is zoned for agricultural use and communal grazing because of its relatively rich nutrient content. Cattle grazing, goat browsing and fire activities have negative impact on the herbaceous cover, leading to high proportions of bare ground and exposed soil (Petersen, 2006). Woody vegetation is represented by random anisotropic, forestry double bounce, vegetation (anisotropic particles), dihedral scattering and dipole classes, which are used to produce woody biomass distribution maps.

## Above-ground woody biomass estimates

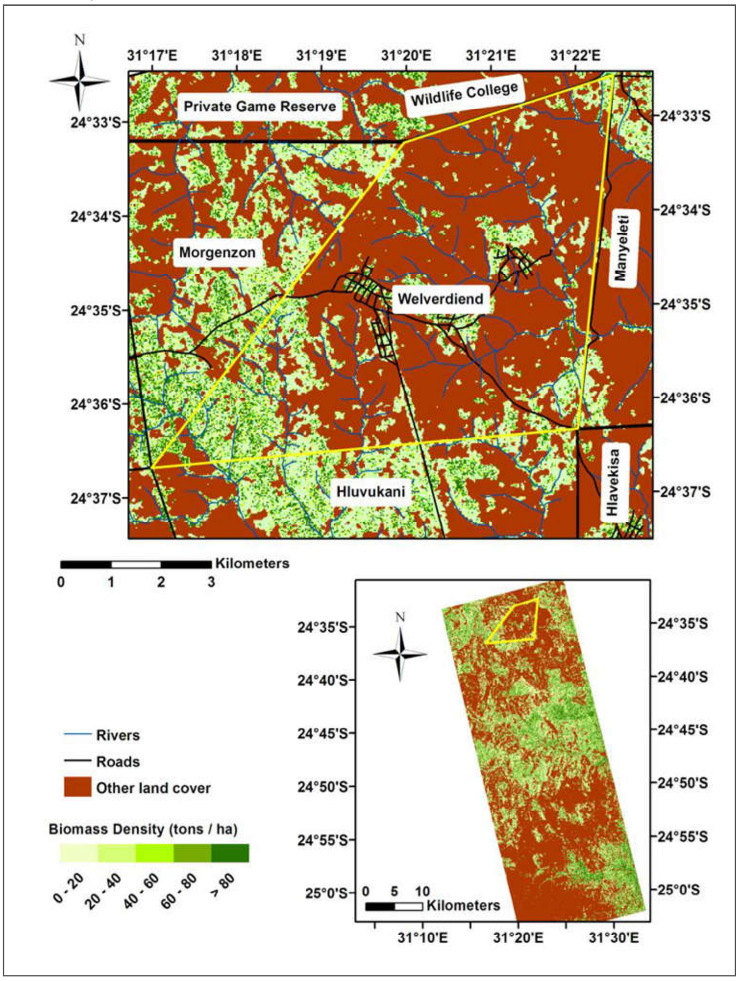


***Figure 4*** ***Above-ground biomass density map of the entire ALOS PALSAR PSR_MMC_TP__0003140001 scene.***

*The area around Welverdiend village used for generating the training data is outlined in the upper region.*

[2] http://www.environment.gov.za/environmetal_management_framework/vegetation.pdf, *accessed on 23 February 2012*

The biomass prediction equations were applied to polarimetric retrievals acquired under wet and dry conditions in Welverdiend village (highlighted in Figure 4 above). The total above-ground woody biomass was estimated at (23 ± 2) x 103 t and (48 ± 8) x 103 t using retrievals acquired in November 2008 (wet condition) and May 2009 (dry condition), respectively. The difference between the estimates (25 x 103 t) was more than twice standard deviation of the estimate (17 x 103 t). The difference may be due to the effect of tree phenology and weather conditions at the time of acquisition on the backscattered signal.

## Discussion

The selection of the site for the field assessment surveys was constrained by the design of the larger VW Foundation BioModels project. The village we selected is in a densely populated rural region characterised by severe degradation of the associated woody biomass. As a result, the field biomass densities (Table 1) do not represent the full range encountered in most savanna woodlands. There are more surveyed plots at the lower end and very few in the medium to higher end of the range. Furthermore, the accuracy of estimating above-ground biomass quantities in surveyed plots was subject to several factors: errors in tree diameter measurements; omission of trees with diameters below a certain minimum; and the accuracy of the allometric equations used for the given woodland (Luckman et al., 1997; Mabowe, 2006; Saatchi et al., 2007a). Moreover, many savanna trees had morphology of multiple stems that branched at ground level, whereas current allometric equations were derived using single stemmed trees that branched well above-ground (Netshiluvhi & Scholes, 2001). We recommend the establishment of site-specific allometric equations to improve the reliability of relationship between biomass estimates and backscatter intensities.

The raw data showed weak correlations (R2 = 0.48 and 0.32) between above ground biomass and HV polarised backscatter intensity for retrievals acquired under wet and dry conditions, respectively. The initial results seemed to imply that there was no robust relationship between backscatter and biomass in the study area. We then applied a bootstrapping approach to mitigate the effects of the limited number of surveyed plots and sampled the training dataset with replacement. The resampled dataset with the highest correlation coefficient was used to determine the best regression equation for each polarisation channel. The results (Table 3) showed that the relationship between above-ground biomass density and sigma nought for the HV polarisation retrievals was consistent across weather (wet and dry) conditions, with R2 values above 63%. This observation is consistent with results from studies in other biomes (Bombelli et al., 2009; Das & Ravindaranth, 2007; Fransson et al., 2007; Leckie, 1998). HH and VV retrievals relate well to above-ground biomass densities under wet conditions due to the effect of moisture on the radar signal interaction with vegetated terrain. Double bounce scattering was more evident because of the moisture content in both soil and tree trunks (Kasischke et al., 1995; Santoro et al., 2005).

The limited number of surveyed plots, coupled with their poor distribution across the range of biomass investigated, presents a weak link in the correlation between the above-ground biomass densities and ALOS PALSAR backscatter intensities. For this reason, the biomass prediction equations presented in this paper are not yet accurate enough for monitoring applications. The equations must be improved by undertaking further field surveys using a larger number of permanent plots to account for variations in seasonal moisture, plant phenology and biomass density variations across the full spectrum of savanna woodlands.

We used polarimetric decomposition and classification algorithms to successfully classify in terms of its scattering mechanism. The woody vegetation classes (random anisotropic, forest double bounce, vegetation (anisotropic), dihedral and dipole scattering mechanisms) were found to be closely related to the interaction of the radar backscatter with the various components of the woody vegetation. These woody vegetation classes were used to map the spatial distribution of above-ground biomass within the precincts of the Welverdiend village. Information about the extent of live woody biomass, coupled with equations that allow estimation of its carbon content, is useful for determining whether woodlands are carbon sources or sinks. Where woodlands are identified as carbon sources, funding from carbon initiatives such as Reducing Emissions from Deforestation and forest Degradation (REDD) may be used to support the transition to modern forms of energy, hopefully resulting in reduced dependence on fuelwood. Improved fire management regimes and appropriate fuelwood harvesting methods, which do not denude vegetation cover while maintaining continuous canopies, are crucial for raising carbon storage capacities of communal woodlands (Thornley & Cannell, 2000). In order to improve carbon estimates at local, national and global scales, it is vital to establish allometric equations for each of the woody vegetation classes derived from polarimetric classification.

## Conclusion

The results presented in this paper demonstrate the potential to map and quantify above-ground woody biomass in semi-open communal African savanna woodlands using full polarimetric spaceborne synthetic aperture radar retrievals. Our approach is particularly useful for woodland practitioners as it provides estimates of available biomass and its spatial distribution. Such information is vital for modelling the accessibility of communal woodlands, mapping the available herbaceous cover for grazing purposes and the inclusion of communal woodlands in global carbon sequestration initiatives. Although full polarimetric acquisitions at L band are not widely available, the approaches developed in this study have laid the foundation for using full polarimetric spaceborne retrievals from spaceborne SAR missions (ALOS PALSAR, ALOS II and BIOMASAR) to map and quantify woody biomass at the local, national and global scales.

## Acknowledgements

Sincere gratitude is extended to the VW Foundation for funding this work through the "Modelling of the domestic energy system based on biomass energy in rural areas in southern Africa - BioModels" project. We like to applaud the assistance rendered by Ludger Eltrop, Uli Fahl of IER, and Timon Wehnert and Michael Knoll of IZT in facilitating the VW BioModels project. We are grateful to the European Space Agency (ESA) for providing the ALOS PALSAR full polarimetric data under the Principal Investigator Project (CIP.6143) on "Quantifying above ground woody biomass in communal African savanna woodlands using fully polarimetric L-band data". The authors acknowledge Irena Hajnsek and her team (Thomas Busche, Jun Su Kim, Maria, Anna, Daniela and Astos) for the induction course in processing and interpretation of synthetic aperture radar retrievals at the German Aerospace Centre (DLR). We are indebted to Andreas Vollrath and Ralf Knuth from the Friedrich Schiller University, Jena, for their assistance in processing ALOS PALSAR retrievals. We acknowledge financial support from the South African National Research Foundation (NRF), through the Focus Area grant "Sustainability Studies Using GIS & Remote Sensing" (FA2005040600018) and the University of Johannesburg Quick Wins Grant (ANN1-QW008) to Prof. H. Annegarn.

## References

Banks, D. I., Griffin, N. J., Shackleton, C. M., Shackleton, S. E., & Mavrandonis, J. M. (1996). Wood supply and demand around two rural settlements in semi-arid savanna, South Africa. Biomass and Bioenergy, 11(4), 319-331.

Bombelli, A., Avitabile, V., Balzter, H., Marchesini, L. B., Bernoux, Brady, M., M., Hall, R., Hansen, M., Henry, m., Herold, M., Janetos, A., Law, B. E., Manlay, R., Marklund, L. G., Olsson, H., Pandey, D., Saket, M., Schmullius, C., Sessa, R., Shimabukuro, Y. E., Valentini, R., Wulder, M., (2009). Biomass: Assessment of the status of the development of standards for the Terrestrial Essential Climate Variables, Version 10, 25 May 2009. Rome: Global Terrestrial Observing System.

Campbell, B. M., Frost, P., & Byron, N. (1996). Miombo woodlands and their use: overview and key issues. In B. M. Campbell (Ed.), The miombo in transition: woodlands and welfare in Africa. Bogor: Centre for International Forestry Research.

Chidumayo, E. N., Masialeti, I., Ntalasha, H., & Kalumiana, O. S. (2002). Charcoal Potential in Southern Africa Final Report for Zambia. Stockholm: Stockholm Environment Institute.

Cloude, S. R., & Pottier, E. (1997). An entropy based classification scheme for land applications of polarimetric SAR. IEEE Transactions on Geoscience and Remote Sensing, 35, 68-78.

Collins, J. N., Hurtley, L. B., Williams, R. J., Boggs, G., Bell, D., & Bartolo, R. (2009). Estimating landscape scale vegetation carbon stocks using airborne multi-frequency polarimetric synthetic aperture radar (SAR) in savannahs of north Australia. International Journal of Remote Sensing, 30(5), 1141-1159.

Das, S., & Ravindaranth, N. H. (2007). Remote sensing techniques for biomass production and carbon sequestration projects. In F. Rosillo-Callé, P. de Groot, S. L. Hemstock & J. Woods (Eds), The biomass assessment handbook (pp. 178-193): Earthscan.

Fransson, J. E. S., Magnusson, M., Folkesson, K., Hallberg, B., Sandberg, G., Smith-Jonforsen, G., Gustavsson, A., & Ulander, L.M.H. (2007). Mapping of wind-thrown forests using VHF/UHF SAR images. IEEE Explore: Geoscience and Remote Sensing Symposium, 2007. IGARSS 2007, pp. 2350-2353.

Freeman, A., & Durden, S. L. (1998). A three component scattering model for polarimetric SAR data. IEEE Transactions on Geoscience and Remote Sensing, 36(3), 963-973.

Ghilani, C. D., & Wolf, P. R. (2008). Elementary surveying: an introduction to Geomatics (12th edition). New York: Pearsons.

Kasischke, E. S., Christensen Jr., N. L., & Bourgeau-Chavez, L. L. (1995). Correlating radar backscatter with components of biomass in Loblolly pine forests. IEEE Transactions on Geoscience and Remote Sensing, 33(3), 643-659.

Knuth, R. (2008). Evaluation of the useability of full polarimetric ALOS PALSAR data for a forest/nonforest discrimination of the tropical rain forest in the Democratic Republic of Congo. Unpublished MSc thesis, Freidrich-Schiller-University Jena, Germany.

Lauknes, I., & Malnes, E. (2004). Automatical geocoding of SAR products. Proc. of the 2004 Envisat & ERS Symposium, Salzburg, Austria, 6-10 September 2004 (ESA SP-572, April 2005) 6 pp.

Le Toan, T., Quegan, S., Woodward, I., Lomas, M., Delbart, N., & Picard, G. (2004). Relating radar remote sensing of biomass to modelling of forest carbon budgets. Climate Change, 67, 379-402.

Leckie, D. G. (1998). Forest applications using imaging radar. In F. M. Henderson & A. J. Lewis (Eds), Manual of remote sensing - principles and applications of imaging radar (3rd edition, Vol. 2, pp. Tsh435-509): Wiley.

Lee, J.-S., & Pottier, E. (2009). Polarimetric Radar Imaging - from Basics to Applications. Boca Raton, FL: CRC Press.

Liang, P., Moghaddam, M., Pierce, L. E., & Lucas, R. M. (2005). Radar backscattering model for multilayer mixed-species forests. IEEE Transactions on Geoscience and Remote Sensing, 43(11), 2612-2626.

Lu, D. (2006). The potential and challenge of remote sensing-based biomass estimation. International Journal of Remote Sensing, 27(7), 1297-1328.

Lucas, R. M., Cronin, N., Lee, A., Moghaddam, M., Witte, C., & Tickle, P. (2006). Empirical relationships between AIRSAR backscatter and LiDAR-derived forest biomass, Queensland, Australia. Remote Sensing of Environment 100, 407-425.

Lucas, R. M., Moghaddam, M., & Cronin, N. (2004). Microwave scattering from mixed species forests, Queensland, Australia. IEEE Transactions on Geoscience and Remote Sensing, 42(10), 2142-2159.

Lucas, R. M., Tickle, P., Lee, A., Austin, J., Witte, C., Jones, K., Cronin, N., Moghaddam, M., & Milne, A. K (2002). Use of AIRSAR (POLSAR) data for quantifying the biomass of woodlands, Queensland, Australia. (11 February 2010). Retrieved from http://airsar.jpl.nasa.gov/documents/workshop2002/papers/P6.pdf

Luckman, A., Baker, J., Kuplich, T. M., Yanasse, C. F., & Frery, A. C. (1997). A study of the relationship between radar backscatter and regenerating tropical forest biomass for spaceborne SAR instruments. Remote Sensing of Environment, 60(1), 1-13.

Mabowe, B. R. (2006). Aboveground biomass assessment in Serowe woodlands, Botswana. Unpublished MSc thesis, ITC, The Netherlands, Enschede.

Milne, A. K., Lucas, R. M., Cronin, N., Dong, Y., & Witte, C. (1999). Monitoring biomass using polarimetric multi-frequency SAR In Å. Rosenqvist, M. Imhoff, A. Milne & C. Dobson (Eds.), Remote Sensing and the Kyoto Protocol: a review of available and future technology for monitoring treaty compliance. Ann Arbor, MI: ISPRS.

Mitchard, E. T. A., Saatchi, S. S., Woodhouse, I. H., Nangendo, G., Ribeiro, N. S., Williams, M., Ryan, C. M., Lewis, S. L., Feldpausch, T. R., & Meir, P. (2009). Using satellite radar backscatter to predict above-ground woody biomass: A consistent relationship across four different African landscapes. Geophysical Research Letters, 36. L23401, doi:10.1029/2009GL040692.

Moore, D. S., McCabe, G. P., & Craig, B. A. (2009). Introduction to the Practice of Statistics (6th edition). New York NY: W. H. Freeman.

Mutanga, O., H. Prins, H. T., Skidmore, A. K., van Wieren, S., Huizing, H., Grant, R. Peel, M., & Biggs, H. (2004), Explaining grass-nutrient patterns in a savanna rangeland of southern Africa, Journal of Biogeography, 31, 819-829.

Mutanga, O., Skidmore, A. K., Kumar, L., & Ferwerda, J. (2005). Estimating tropical pasture quality at canopy level using band depth analysis with continuum removal in the visible domain. International Journal of Remote Sensing, 26(6), 1093-1108.

Nangendo, G. (2005). Changing Forest-Woodland-Savanna mosaics in Uganda: Implications for conservation. PhD thesis, Wageningen University; ITC Dissertation number 123, International Institute for Geo-information Science & Earth Observation, Enschede, The Netherlands, ISBN 90-8504-163-5; 139 pp.

Narvaes, I. S., Silva, A. Q., & Santos, J. R. (2007,). Evaluation of the interaction between SAR L-band signal and structural parameters of forest cover. IEEE International Geoscience and Remote Sensing Symposium IGARSS 07, Barcelona, Spain., IEEE Explore, IGARSS 07, pp. 1607-1610.

Netshiluvhi, T. R., & Scholes, R. J. (2001). Allometry of South Africa woodland trees. Pretoria: CSIR.

Petersen, L. M. (2006), Granivores as ecosystem regulators of woody plant increasers in semi-arid Savannas of the Lowveld, South Africa, MSc thesis, University of the Western Cape, Cape Town.

Prakoso, K. U. (2006). Tropical forest mapping using Polarimetric and Interferometric SAR data - a case study of Indonesia. Unpublished PhD thesis, Wageningen University, The Netherlands.

Rauste, Y. (2005). Techniques for Wide-Area Mapping of Biomass Using Radar Data,, Doctor of Technology thesis, Helsinki University of Technology, and Espoo, Finland: VTT Publications.

Richards, J. A., & Jia, X. (2006). Remote Sensing Digital Image Analysis (4th edition). Berlin: Springer.

Riedel, T., Thiel, C., & Schmullius, C. (2008). Fusion of multispectral optical and SAR images towards operational land cover mapping in Central Europe. In T. Blaschke, S. Lang & G. J. Hay (Eds), Object-Based Image Analysis Berlin Heidelberg: Springer, pp. 493-511.

Rutherford, M. C., Mucina, L., Lötter, M. C., Bredenkamp, G. J., Smit, J. H. L., Scott Shaw, C. R., Hoare, D. B., Goodman, P. S., Bezuidenhout, H., Scott, L., Ellis, F., Powrie, L. W., Siebert, F., Mostert, T. H., Henning, B. J., Venter, C. E., Camp, K. G. T., Siebert, S. J., Matthews, W. S., Burrows, J. E., Dobson, L., van Rooyen, N., Schmidt, E., Winter, P. J. D., du Preez, P. J., Ward, R. A., Williamson S. & Hurter, P. J. H. (2006). Savanna Biome. In L. Mucina, & M. C. Rutherford, (Eds) 2006. The vegetation of South Africa, Lesotho and Swaziland. Strelitzia 19, pp. 438-538. Pretoria: South African National Biodiversity Institute.

Ryan, C. M., Hill, T., Woollen, E. Ghee, C., Mitchard, E., Cassels, G., Grace, J., Woodhouse, I. H., & Williams M. (2011), Quantifying small scale deforestation and forest degradation in African woodlands using radar imagery, Global

Change Biology, doi: 10.1111/j.1365-2486.2011.02551.x, 15 pp.

Saatchi, S., Halligan, K., Despain, D. G., & Crabtree, R. L. (2007a). Estimation of forest fuel load from radar remote sensing. IEEE Transactions on Geoscience and Remote Sensing, 45(6), 1726-1740.

Saatchi, S. S., Houghton, R. A., Dos SantosAlvala, R. C., Soares, J. V., & Yu, Y. (2007b). Distribution of aboveground live biomass in the Amazon basin. Global Change Biology, 13, 816–837.

Santoro, M., Askne, J., & Dammert, P. B. G. (2005). Height influence of RES interferometric phase in boreal forest. IEEE Transactions on Geoscience and Remote Sensing, 43(2), 207-217.

Santoro, M., Eriksson, L., Askne, J., & Schmullius, C. (2006). Assessment of stand-wise stem volume retrieval in boreal forest from JERS-1 L-band SAR backscatter. International Journal of Remote Sensing, 27(16), 3425-3454.

Santoro, M., J. E. S. Fransson, L. E. B. Eriksson, M. Magnusson, L. M. H. Ulander and H. Olsson (2009), Signatures of ALOS/PALSAR L-band backscatter in Swedish forest, IEEE Transactions on Geoscience and Remote Sensing, 47(12), 4001-2019.

Santos, J. R., Pardi Lacruz, M. S., Araujo, L. S., & Keil, M. (2002). Savanna and tropical rainforest biomass estimation and spatialization using JERS-1 data. International Journal of Remote Sensing, 23(7), 1217-1229.

Scholes, R. J. (1997). Savanna. In R. M. Cowling, D. M. Richardson & S. M. Pierce (Eds), Vegetation of Southern Africa. Cambridge, Cambridge University Press, pp. 258-277.

Scholes, R. J., & Archer, S. R. (1997). Tree-grass interaction in savannas. Annual Review of Ecology and Systematics, 28, 517-544.

Thornley, J. H. M., & Cannell, M. G. R. (2000), Managing forests for wood yield and carbon storage: a theoretical study, Tree Physiology, 20, 477-484.

Touzi, R., Boerner, W. M., Lee, J. S., & Lueneburg, E. (2004). A review of polarimetry in the context of synthetic aperture radar: concepts and information extraction. Canadian Journal of Remote Sensing, 30(3), 380-407.

Uren, J., & Price, W. F. (2010). Surveying for Engineers,(10th edition): Basingstoke, Hampshire: Palgrave Macmillan.

Van Zyl, J. J. (1989). Unsupervised classification of scattering mechanisms using radar polarimetry data. IEEE Transactions on Geoscience and Remote Sensing, 27, 36–45.

Viergever, K. M. (2008). Establishing the sensitivity of Synthetic Aperture Radar to above ground biomass in wooded savannas. Unpublished PhD thesis, University of Edinburgh, Edinburgh.

Viergever, K. M., Woodhouse, I. H., & Stuart, N. (2007). Backscatter and interferometry for estimating above-ground biomass in tropical savanna woodland. Geoscience and Remote Sensing Symposium, 2009, Barcelona. IEEE Explore, IGARSS 2009, Volume: 3, pp. III-1047 - III-1050.

VON MALTITZ, G. P., & SCHOLES, R. J. (1995). The burning of fuelwood in South Africa: When is it sustainable? . Environmental Monitoring and Assessment 38, 243-251.

WATANABE, W., SHIMADA, M., ROSENQVIST, A., TADONO, T., MATSUOKA, M., ROMSHOO, S. A., OHTA, K., FURUTA, R., NAKAMURA, K., & MORIYAMA, T. (2006). Forest structure dependency of the relation between L-band sigma nought and biophysical parameters. IEEE Transactions on Geoscience and Remote Sensing, 44(11), 3154-3165.

WERNER, C., STROZZI, T., WEGMÜLLER, U., & WIESMANN, A. (2002). SAR geocoding and multi-sensor image registration. Geoscience and Remote Sensing Symposium, IGARSS '02. IEEE Explore, IGARSS'02, Volume: 2, 902-904.

WHITE, F. (1983). Vegetation Map of Africa. Paris: United Nations Educational, Scientific and Cultural Organisation.

WOODHOUSE, I., CASSELLS, G., MITCHARD, E., & TEMBO, M. (2009, 12-17 JULY). The use of ALOS PALSAR for supporting sustainable forest use in Southern Africa: a case study in Malawi. Geoscience and Remote Sensing Symposium, IGARSS '09. IEEE Explore, IGARSS'09, Volume: 2, II-206 - II-209.

YAMAGUCHI, Y., YAJIMA, Y., & YAMADA, H. (2005). Four-component scattering model for polarimetric SAR image decomposition. IEEE transactions on Geoscience and Remote Sensing, 43(8), 1699-1706.

ZHANG, L., ZHANG, J., ZOU, B., & ZHANG, Y. (2008). Comparison of methods for target detection and applications using Polarimetric SAR image. PIERS Online, 4(1), 140-145.